

Title Page

**Novel small molecule inhibitors of TLR7 and TLR9:
mechanism of action and efficacy *in vivo***

Marc Lamphier, Wanjun Zheng, Eicke Latz, Mark Spyvee, Hans Hansen, Jeffrey Rose,
Melinda Genest, Hua Yang, Christina Shaffer, Yan Zhao, Yongchun Shen, Carrie Liu, Diana
Liu, Thorsten R Mempel, Christopher Rowbottom, Jesse Chow, Natalie C. Twine, Melvin Yu,
Fabian Gusovsky, Sally T. Ishizaka

Eisai Inc., 4 Corporate Drive, Andover MA, 01810 (M.L., W.Z., M.S., H.H., J.R., M.G., H.Y.,
C.S., J.Z., Y.S., C.L., D.L., C.R., J.C., N.C.T., M.Y., F.G., S.T.I.)

Department of Infectious Diseases and Immunology, University of Massachusetts, Worcester,
MA and Institute of Innate Immunity, University of Bonn, Germany (E.L.)

Center for Immunology and Inflammatory Diseases and Center for Systems Biology,
Massachusetts General Hospital and Harvard Medical School, Charlestown, MA, USA.
(T.R.M)

Running Title Page

Running Title: Small Molecule TLR Inhibitors

Corresponding Author:

Sally T. Ishizaka
Phone: 978-837-4642
Fax: 978-837-4932
E-mail: sally_ishizaka@eisai.com

Text pages: 22 pages
Tables: 2 tables
Figures: 10 figures
References: 33 references
Abstract: 232 words
Introduction: 567 words
Discussion: 939 words

Non-standard abbreviations:

ANA	anti-nuclear antibodies
BMDCs	Mouse bone marrow-derived dendritic cells
dsDNA	double-stranded DNA
FITC	Fluorescein isothiocyanate
IL-6	Interleukin-6
LPS	lipopolysaccharide endotoxin
PAMPA	Parallel Artificial Membrane Assay
PBMCs	peripheral blood mononuclear cells
PE	phycoerythrin
pIC	poly inosine-cytosine
SLE	Systemic Lupus Erythematosus
TLR	Toll-like receptor

Abstract

The discovery that circulating nucleic acid-containing complexes in the serum of autoimmune lupus patients can stimulate B cells and plasmacytoid dendritic cells via Toll-like receptors 7 and 9 suggested that agents that block these receptors might be useful therapeutics. We identified two compounds, AT791 and E6446, that inhibit TLR7 and 9 signaling in a variety of human and mouse cell types, and inhibit DNA - TLR9 interaction *in vitro*. When administered to mice, these compounds suppress responses to challenge doses of CpG-containing DNA, which stimulates TLR9. When given chronically in spontaneous mouse lupus models, E6446 slowed development of circulating anti-nuclear antibodies and had a modest effect on anti-double stranded DNA (dsDNA) titers, but showed no observable impact on proteinuria or mortality. We discovered that the ability of AT791 and E6446 to inhibit TLR7 and 9 signaling depends on two properties: weak interaction with nucleic acids and high accumulation in the intracellular acidic compartments where TLR7 and 9 reside. Binding of the compounds to DNA prevents DNA - TLR9 interaction *in vitro* and modulates signaling *in vivo*. Our data also confirms an earlier report that this same mechanism may explain inhibition of TLR7 and 9 signaling by hydroxychloroquine (Plaquenil), a drug commonly prescribed to treat lupus. Thus, very different structural classes of molecules can inhibit endosomal TLRs by essentially identical mechanisms of action, suggesting a general mechanism for targeting this group of TLRs.

Introduction

The Toll-like Receptors (TLRs) recognize a wide array of pathogen-associated and endogenous molecular patterns that trigger innate immune responses (reviewed in Sasai and Yamamoto, 2013). Certain types of nucleic acids can provoke a robust innate immune response, and this recognition is mediated by cytoplasmic receptors such as RIG-I and AIM2 and by TLRs localized inside endosomes and lysosomes (Barbalat et al, 2011). The nucleic acid-recognizing TLRs include TLR3, which is activated by double-stranded RNAs, TLRs 7 and 8, which are activated by single-stranded RNAs and TLR9, which mediates responses to single-stranded DNAs. The intracellular localization of these TLRs appears to prevent their spontaneous activation by circulating nucleic acids (Barton et al, 2006), however under certain pathological conditions endogenous nucleic acids can overcome this barrier. The immune complexes found in sera of patients suffering from systemic lupus erythematosus (SLE) typically contain nucleic acids associated with various proteins such as antibodies, the chromatin-associated protein HMGB1, the antimicrobial peptide LL39, ribonuclear proteins and others. These associated proteins may protect the bound nucleic acid from degradation and/or facilitate their entry into the cell, as is the case for Fc receptor-mediated uptake of antibody-nucleic acid complexes (Leadbetter et al., 2002, Means et al, 2005). Once inside the endolysosomal compartments, the nucleic acid cargo can then stimulate the intracellular TLRs, priming the immune system for further generation of anti-self antibodies. This cycle of innate immune recognition, generation of self-antibodies, and enhanced immune complex formation is believed to contribute to the pathogenesis of SLE and possibly Sjogren's syndrome (Marshak-Rothstein et al., 2006), a finding confirmed in animal models treated with TLR7 and TLR9-competitive antagonist oligonucleotides (Barrat et al., 2007; Christensen et al., 2005). In addition, TLR-mediated pathological responses to nucleic acids may contribute to other pathologies, such as damage due to liver injury or lung infection,

MOL #89821

pancreatitis, and graft-versus-host disease (Bamboate et al., 2010, Calcaterra et al., 2008, Hoque et al., 2011, Itagaki, 2011). Recent clinical data show that an injectable, synthetic, competitive oligonucleotide inhibitor of TLR9 has efficacy in psoriasis (Kimball et al., 2013).

The purpose of our work was to develop an orally available, non-oligonucleotide small molecule inhibitor of TLR9. We describe two small molecules, AT791 and E6446, that can potentially inhibit not only TLR9 stimulation by DNA, but also block TLR7 stimulation by RNA in mouse cell lines and inhibit DNA-TLR9 interaction *in vitro*. These compounds are orally bioavailable in mice, and can inhibit short-term induction of inflammatory cytokines by DNA. In a mouse MRL/lpr spontaneous model of lupus, E6446 slowed the development of circulating anti-nuclear antibodies and modestly suppressed anti-dsDNA titers, although it showed no observable impact on proteinuria or mortality. E6446 has also recently been shown to be effective in preventing hyper-inflammation and lethality caused by the parasite *Plasmodium berghei* in a mouse model of cerebral malaria (Franklin et al, 2011).

As described in an earlier preliminary report (Ishizaka, 2008), we show here that these compounds utilize an unusual mechanism of action: they interact weakly with nucleic acids but accumulate to a sufficiently high concentration in acidic compartments in cells that this interaction becomes significant. We also observed that the antimalarials hydroxychloroquine and chloroquine utilize a similar mechanism to suppress TLR7 and 9, consistent with a recent report by Kuznik et al (2011). Thus, very different structural classes of molecules can inhibit endosomal TLRs by essentially identical mechanisms of action, suggesting a general mechanism for targeting this group of TLRs.

Materials and Methods

Animals. Female BALB/c, were obtained from Charles River Laboratories or Jackson Laboratories and DO11.10 and MRL/lpr-MpJ mice from Jackson Laboratories, and housed under standard conditions. All animal experimental work was performed under protocols approved by the Eisai Andover IACUC.

Reagents and Compounds. AT791 (3-(4-(6-(3-(dimethylamino)propoxy)benzo[d]oxazol-2-yl)phenoxy)-N,N-dimethylpropan-1-amine) and E6446 (6-(3-(pyrrolidin-1-yl)propoxy)-2-(4-(3-(pyrrolidin-1-yl)propoxy)phenyl)benzo[d]oxazole) were synthesized at Eisai Inc. and their structures are shown in Figure 1A. Hydroxychloroquine and chloroquine were purchased from Sigma (St. Louis, MO). Soluble TLR9-Fc was cloned, expressed in HEK cells, and purified as previously described (Latz et al., 2004). LPS was purchased from List Biological Laboratories or Sigma. R-848, CL-097 and Cytoxan was from Sigma. Monoclonal antibodies to dsDNA (clone BV 16-13) were from Millipore.

Oligonucleotides. Phosphothioate-modified DNA or RNA oligonucleotides were obtained from Sigma Genosys or Dharmacon. Sequences (5' to 3'): **CpG2006** (TCG TCG TTT TGT CGT TTT GTC GTT), **3X-CpG2006** (a 3x concatamer of CpG2006), **CpG2216** (GGG GGA CGA TCG TCG GGG GG), **GpC2216** (GGG GGA GCA TGC TGC GGG GG), **CpG1668** (TCC ATG ACG TTC CTG ATG CT), **CpG1417** (TCG TCG TTT TGT CG), **RNA40** (GCC CGU CUG UUG UGU GAC UC), **SL4 RNA** (GGG GGA CUG CGU UCG CGC UUU CCC CU). In some cases, RNA oligos were complexed with the cationic lipid DOTAP (Roche) to facilitate uptake by cells (Hemmi et al., 2004)

In Vitro Cell-Based Assessment. HEK293 fibroblast cells (American Type Culture Collection, Manassas, VA) containing an NF- κ B-luciferase reporter were stably transfected with pcDNA3.1D/V5-His-TOPO plasmid (Life Technologies) expressing human TLR9 (directly inserted as a *Taq* polymerase-amplified PCR product) or TLR7 (vector pCMV6-XL5 expressing human TLR7 cDNA from Origene). RAW 264.7 cells were stably transfected with a lentivirus containing an NF- κ B-luciferase reporter (SA Biosciences). Compounds were added to cells 30 min. before stimulation with phosphothioate-modified CpG DNA or RNA oligonucleotides, the small-molecule imidazoquinoline TLR7 agonists R-848 or CL-097, or the TLR4 agonist lipopolysaccharide (LPS). Luciferase reporter activity was assayed using Steadylight (Perkin-Elmer). HEK:TLR7 respond to the imidazoquinoline TLR7 agonists, but not to RNA/DOTAP complexes. RAW cells respond to DNA, RNA (with or without DOTAP), R-848, CL-097 and LPS. For oligonucleotide uptake experiments, RAW 264.7 cells were incubated for 15 minutes with biotinylated CpG2006 complexed to phycoerythrin-streptavidin (BD Biosciences), washed and then fluorescence was visualized by confocal microscopy (Leica SP5).

Primary Cell Assays. Compounds were assayed for the suppression of BALB/c mouse spleen IL-6 production in response to stimulation by oligonucleotide CpG1668. Each compound was added to dissociated splenocytes (5×10^5 per well in complete RPMI/10% FBS in a 96 well plate) before addition of TLR agonists. Cells were stimulated for 72 hrs and supernatants were removed for ELISA analysis of IL-6 (R&D Systems). Mouse bone marrow-derived dendritic cells (BMDCs) were generated by culturing BALB/c marrow cells in RPMI containing 100ng/ml Flt3 ligand for 7 days. 1×10^5 cells in 50ul were assayed for IL-6 production after overnight or 24 hour stimulation with various TLR ligands. For studies using human peripheral blood mononuclear cells (PBMCs), Ficoll-separated mononuclear

MOL #89821

cells were isolated from healthy volunteer donors, washed, and plated with stimulatory oligonucleotide CpG2216 in complete RPMI for 72 hrs. Interferon in supernatant was quantified by ELISA (Pestka Biomedical Laboratories).

Antigen Presentation Assay: Splenocytes were isolated from DO11 mice, washed twice after RBC lysis and re-suspended with complete RPMI. 5×10^5 cells/well were seeded in a 96-well plate, with 10 ng/ml OVA323-339 peptide (ISQAVHAAHAEINEAGR, MW 1773.9) or 300 μ g/ml OVA protein (Sigma, MW 42.7 kDa) and serial dilutions of compound. The cells were cultured at 37°C, 5% CO₂ for 48 hours. 150 μ l/well supernatant was harvested and stored at -80°C for IL-2 ELISA. 100 μ l lysis/substrate solution of ATPLite (PerkinElmer) was added into each well. The plate was incubated at dark for 10 min. at room temperature and luminescence measured with an Envision Plate Reader (PerkinElmer).

Microarray analysis E6446 (250nM or 1250nM) or media were added to wells containing 4×10^6 BDMCs. Cells were stimulated with 250nM CpG1668 or left untreated. After 4 hours, cells were harvested and total RNA was isolated using Qiagen RNeasy Mini Kit. GeneChip assay was performed using the Affymetrix Mouse Genome 430A 2.0 Array following the Affymetrix standard eukaryotic target preparation protocol using 1 μ g of total RNA. Array data was normalized using standard RMA GeneData Refiner workflow. All statistical analyses were calculated in GeneData Analyst. All probes were filtered based on arithmetic mean with a threshold at a signal of 100 across all samples. A two-group sample comparison test using a standard t-test was performed between CpG stimulated samples vs. medium control. All genes that were significantly regulated by CpG (uncorrected p-value ≤ 0.05 and fold change ≥ 2) were reported, which included a total of 616 probe sets. Eight probe sets did not map to any known gene with the remaining mapping to a total of 461 known gene symbols. Comparisons between all treatments with medium control were performed. Relative

MOL #89821

normalization method was applied to all the samples relative to the reference group (medium control). Two-dimensional hierarchical clustering using the 616 probe set signature was performed using GeneData Analyst using Manhattan distance and complete linkage.

Antibody-DNA complexes. Plasmid DNA (pcDNA3.1) was linearized with DdeI restriction enzyme and incubated with anti-DNA monoclonal antibody (Chemicon MAB030; clone BV 16-13) for 30 minutes in media before adding to wells containing 50,000 BMDCs. Cells were incubated overnight, and IL-6 was assayed the next day. Anti-biotin antibody (Jackson Labs) was used as a control antibody.

DNA uptake assay. RAW 264.7 cells (1×10^5 cells) were added to wells of a 96-well plate with glass cover slip bottoms (Mattek) and cultured overnight. One hour prior to stimulation, plates were pre-incubated at 4 °C, 37 °C, or 37 °C in the presence of 1 μ M AT791 or E6446. Biotinylated CpG2006 and streptavidin-linked phycoerythrin (PE) were mixed at a molar ratio of 8:1 (DNA:PE), and added to a final concentration of 200nM CpG2006/25nM PE and plates were further incubated at 4 °C or 37 °C. After 30 minutes, wells were washed with cold PBS and cells visualized by confocal microscopy.

Intracellular pH assay RAW 264.7 cells were incubated for 6 hours with 10 mg/ml of a mixture of fluorescein- and pHrodoRed- labelled ~ 10,000 MW dextrans (Life Technologies). Cells were washed 3X in Hank's buffer and AT791 (200nM), E6446 (200nM) or bafilomycin (10nM) were added for one hour. Cells were next visualized by confocal microscopy (Leica SP5). Fluorescein isothiocyanate (FITC; ex488/em525) and pHrodoRed (em563/ex585) fluorescence within intracellular vesicles were quantitated by intensities across line profiles.

After background subtraction, FITC:pHrodo intensity ratios of individual peaks ($n > 20$) were calculated and averaged.

TLR9 – DNA interaction assay. Interaction between 20nM biotinylated CpG2006 oligonucleotide and 5 $\mu\text{g/ml}$ Fc-tagged ectodomain of TLR9 was assayed using an Amplified Luminescent Proximity Homogeneous Assay system (ALPHA-Screen, Perkin-Elmer), as described in Latz et al. (2007). Assays were performed in pH5.5 acetate buffer, 150mM NaCl. Oligo CpG1417 is a 14-nucleotide DNA oligomer that does not detectably interact with Fc-TLR9 in this assay (data not shown).

Compound-DNA interaction. Fluorescence spectroscopy (Hitachi F-2000) was used to monitor the intrinsic fluorescence of 100nM AT791 or E6446 in 50mM NaAce buffer (pH5.5), 150mM NaCl at 310nm excitation / 380nm emission. 400nM of 2-aminopurine was used as a control, as this compound has a very similar fluorescence spectra.

Hydroxychloroquine and chloroquine (5 μM each) fluorescence were monitored in 50mM phosphate buffer (pH 7.2), 150mM NaCl at 330nm excitation / 375nm emission. pH7.2 was used as these compounds fluoresce poorly at lower pH. Various concentrations of CpG2006 DNA or RNA40 oligonucleotides were added to compound solutions, and the change in compound fluorescence as a function of DNA or RNA concentration was analyzed by non-linear regression analysis for fit to a one-site binding curve (GraphPad Prism). DNA interaction with AT791 and E6446 was also quantified using a plate-based equilibrium dialysis system (RED system; Pierce). Compounds (200nM) were added to two chambers separated by an 8kDa cutoff membrane and DNA (3X-CpG2006; 22kDa) was added at various concentrations to one of the chambers. After incubation overnight, the concentrations of compounds in each chamber were quantified by mass spectroscopic analysis, and this data

was analyzed by non-linear regression analysis similar to above.

Intracellular localization of compounds

For the visualization of intracellular AT791 and E6446, HEK293 cells were incubated with 1 μ M of each compound for 5-15 min at 37 °C. The cells were then imaged using a Prairie Ultima IV multiphoton microscope system equipped with an Olympus 60x/1.15 numerical aperture water-immersion lens, and with a MaiTai HP and a MaiTai DeepSee laser (Spectra-Physics/Newport) providing excitation light at 920 nm and 707 nm, respectively. The HEK cells used in these experiments had been retrovirally transduced to stably express either Smad2-EGFP as a cytoplasmic marker or LAMP-1 fused to EGFP as a lysosomal marker. AT791 was also visualized in cervical carcinoma C33A and CV-1 fibroblast cells by conventional confocal microscopy using a UV 351 nm laser ((Leica LSM SP2, courtesy of Owen Schwartz, NIH). Intracellular compound concentration was estimated by comparison to fluorescence obtained with known concentrations of AT791 spotted on microscope slides in pH5.5 buffer.

Parallel Artificial Membrane Permeation Assay (PAMPA). Five μ l of a solution of 2% *L*- α -phosphatidylcholine in dodecane was deposited per well on membranes of a 96-well MultiScreen Permeability plate (Millipore; MAIPN4510). AT791 (10 μ M), E6446 (10 μ M), hydroxychloroquine (40 μ M) or chloroquine (40 μ M) were added to one of the two compartments in pH 5.5 buffer (50 mM NaAce, 150mM NaCl) or pH 7.4 buffer (50mM KPO₄, 150mM NaCl), and the plate was incubated at 37 °C. The next day, compound concentrations in both chambers were quantitated. In one variation of this experiment, 5 μ M AT791 or E6446 was added to both chambers, one of which contained pH5.5 buffer and the other pH7.4 buffer. The redistribution of compound between the two chambers was

monitored for 8 hours.

Drug Treatment in Oligo Challenge. Drug was dissolved in acidified water and administered orally (20mg/kg) 18 hours prior to subcutaneous challenge with CpG1668 (60 µg/head). Two hours after oligo challenge, blood was collected for measurement of IL-6 in serum. IL-6 ELISA kits from BD Bioscience were used according to manufacturer's instructions.

Drug Treatment in Spontaneous Lupus Models. MRL/lpr mice were dosed orally five times a week with 20mg/kg or 60mg/kg E6446 or 60 mg/kg hydroxychloroquine beginning at 5 weeks of age. Cytoxan was administered at 50 mg/kg i.p. every 10 days. A serum sample was taken immediately before the beginning of treatment to monitor changes in autoreactive antibodies. Subsequently serum samples were collected approximately monthly and analyzed for anti-dsDNA by ELISA after 1:500 dilution (Alpha Diagnostics). Body weights and urine samples were taken at the same interval, and proteinuria assessed by ChemStrips (Roche Diagnostics). Anti-nuclear antibodies (ANA) were assessed using commercially available HEp2 slide kits (Antibodies, Inc., Davis, CA), with serum diluted to 1:100 in kit buffer. ANA scores were read blinded.

Results

Inhibition of TLR9 and TLR7 signaling by small molecule ligands

HEK293 cells expressing cloned human TLR9 and an NF-κB:luciferase reporter (HEK:TLR9 cells) were used to screen a compound library for small molecules that could suppress induction of NF-κB by stimulatory DNA (CpG2006). AT791 and E6446 (Fig. 1A) potently suppressed DNA stimulation of HEK:TLR9 cells, with EC50s of 40nM and 10nM,

MOL #89821

respectively, but were significantly less effective at suppressing lipopolysaccharide endotoxin (LPS) stimulation of HEK:TLR4 cells (Table I) or R848 stimulation of HEK:TLR7 cells.

Dendritic cells play a critical role in the initial innate immune response leading to adaptive immunity. We therefore tested the ability of AT791 and E6446 to suppress induction of IL-6 by various TLR ligands in mouse bone marrow-derived dendritic cells (BMDC). As shown in Figure 1B, AT791 and E6446 potently inhibited IL-6 production induced by CpG2216, but were ineffective against induction by the TLR3 ligand poly inosine-cytosine (pIC).

Surprisingly however, the ability of these compounds to suppress TLR7 was ligand-dependent: both AT791 and E6446 were potent inhibitors of IL-6 induction by RNA, but relatively poor inhibitors of IL-6 induction by the small molecule imidazoquinoline ligand R-848. Similar results were seen in mouse splenocytes (Table I). In human PBMCs, AT791 and E6446 could suppress both IL-6 and α -interferon production induced by CpG oligo (Table I). Thus, antagonism is observed across species and output cytokine responses. E6446 showed a modest but consistent superiority over AT791, and both were significantly more potent than hydroxychloroquine (Plaquenil), which is commonly prescribed in the treatment of lupus.

To better understand this antagonism, we examined mRNA expression in BMDCs by microarray analysis. Stimulation with CpG1668 for 4 hours caused a reproducible change in a large number of genes, many of which are involved in inflammation, NF- κ B signaling or the interferon response, consistent with previous reports (Klaschik et al., 2007). Significantly, 250nM and 1.25 μ M E6446 completely suppressed all of the CpG oligo-induced changes in gene expression (Supplemental Figure 1 & Supplemental Data I), while these concentrations of E6446 alone had no observable effect on gene expression after 4 hours. This suggests that

the compound acts at or upstream of signal initiation.

Inhibition of stimulation by immune complexes

Complexes of antibodies with DNA, RNA, chromatin and/or associated proteins are believed to be responsible for the aberrant induction of inflammatory cytokines in lupus patients, as demonstrated by the ability of immune complexes isolated from lupus patients to stimulate TLR7 and TLR9 in cell culture (Vallin et al, 1999, Means et al., 2005). We generated DNA-antibody complexes by incubating highly-purified plasmid DNA with an anti-DNA monoclonal IgG1 antibody. Neither DNA nor antibody alone significantly induced production of IL-6 in BMDCs, but when pre-incubated together, they synergistically stimulated IL-6 production (Fig. 2A). No stimulation was seen when anti-biotin antibody was substituted for anti-DNA antibody (Fig. 2A) and no stimulation was observed in BMDCs from TLR9 knockout mice (data not shown) Figure 2B shows that immune complex stimulation was inhibited by AT791. Thus, AT791 can inhibit stimulation of TLR9 by DNA-antibody complexes.

Antagonism does not involve inhibition of nucleic acid uptake or modulation of endosomal pH

Mouse RAW 264.7 cells transfected with an NF- κ B-responsive luciferase reporter were stimulated by CpG2006 DNA, SL4 RNA, CL-097 or LPS. Stimulation by CpG2006 or SL4 RNA, but not by LPS or CL-097, was completely suppressed with 100nM of AT791 or E6446 (Fig. 3, left 2 panels). To visualize uptake we generated complexes of biotinylated CpG2006 and streptavidin-linked phycoerythrin (PE-DNA), incubated these with RAW cells, and washed and examined the cells by confocal microscopy. No fluorescence was observed in cells that had been incubated with PE alone (data not shown), but fluorescence appeared as

MOL #89821

intracellular punctate spots in cells incubated PE-DNA complexes at 37 degrees (Fig. 4). When PE-DNA was incubated with cells at 4 degrees, fluorescence was confined to the cell surface. Uptake of PE-DNA could also be blocked by the GTPase inhibitor Dynasore (data not shown). Pre-treatment of cells for 3 hours with 1 μ M AT791 or E6446 did not cause any visible change in subsequent DNA-PE complex uptake or localization.

Since both AT791 and E6446 are weak bases, we investigated whether they inhibit TLR7 and 9 by modulating endosomal pH. First, we compared inhibition by AT791 and E6446 versus known modulators of endosomal pH, bafilomycin, monensin and methylamine. As shown in Figure 3 (center panels), these pH modulators were all effective in inhibiting TLR7 and 9 signaling, however in contrast to AT791 and E6446, they show no selectivity for nucleic acid versus imidazoquinoline ligands. Next, changes in intracellular pH were monitored with dextran (10,000 MW) labeled with fluorescein isothiocyanate (FITC) and pHrodo (Life Technologies). Both of these dyes are pH-sensitive: FITC fluorescence decreases, and pHrodo fluorescence increases as pH decreases over the range pH 7.5 to pH 5.0, and the ratio of FITC:pHrodo fluorescence can be used to indicate pH within this range. After loading with dextran complexes, RAW cells were incubated for ~ 3 to 4 hours with a concentration of each compound that resulted in >95% inhibition in the cell-based reporter assays. Cells were imaged by confocal microscopy and intracellular fluorescence was quantitated along line profiles. The pH modulators bafilomycin, monensin and methylamine produced a clear change in intracellular pH, whereas AT791 and E6446 had no obvious effect (Fig. 5, Supplemental Figure 2). 5 μ M hydroxychloroquine or chloroquine also had no measurable effect on intracellular pH, even though these concentrations can inhibit TLR9 or 7 signaling induced by DNA or RNA ligands, similar to observations reported by Manzel et al. (1999) and Kuznik et al (2011). Finally, we observed that 100nM AT791 had no significant effect on

OVA peptide presentation to DO11 T cells, a process that is inhibited by changes in endosomal pH (Supplemental Figure 3). Taken together, these data indicated that these compounds do not inhibit TLR7 and 9 signaling by modulation of endosomal / lysosomal pH.

DNA – TLR9 interaction assay

We next asked if these compounds could inhibit the interaction between TLR9 and DNA *in vitro*. We used an amplified luminescent proximity homogeneous system (AlphaScreen; Perkin Elmer) to detect an interaction between biotinylated CpG2006 oligonucleotide and the extracellular domain of TLR9 fused to immunoglobulin Fc-TLR9 (Latz et al., 2007), and found that E6446 and AT791 inhibited *in vitro* DNA – TLR9 interaction (Fig.6A). In a separate experiment, these compounds did not inhibit the interaction between Fc-tagged TLR2 and the biotinylated TLR2 ligand PamCysK (data not shown). The concentrations of AT791 and E6446 required to inhibit TLR9-DNA interaction are several orders of magnitude higher than those required to inhibit TLR7 or 9 signaling in cell cultures. However, when we examined a series of analogs of AT791 and E6446, we observed a good correlation between their potencies in the TLR9-DNA interaction assay and the cell-based assay (Supplemental Figure 4), suggesting that the ability of these compounds to disrupt DNA-TLR9 interaction *in vitro* is in some way related to their inhibition of TLR9 signaling.

Identification of drug target

We next asked which of the two components in the DNA-TLR9 interaction assay is the target of the compounds: DNA or TLR9? We imagined that if these compounds interact with DNA, it might be possible to alleviate inhibition by the addition of excess free oligonucleotide, which would compete for binding to the compound. This “oligo decoy” experiment requires that the competing oligonucleotide itself does not interact with TLR9. We identified a

MOL #89821

non-TLR9-binding, non-signaling 14-nucleotide single-stranded oligonucleotide, CpG1417, that could be used as the decoy oligo (see Methods). We started with optimal amounts of biotinylated CpG2006 oligonucleotide and Fc-TLR9, and observed the expected inhibition by 10 μ M AT791 (Fig. 6B). However, when we added increasing amounts of CpG1417, the assay signal increased almost to the non-suppressed level. This data suggests that AT791 inhibits DNA – TLR9 interaction in vitro via an interaction with DNA and not with TLR9.

To confirm whether the interaction of compound with DNA is relevant to its ability to inhibit DNA – TLR9 interaction in cells, we developed a live cell version of the oligo decoy experiment. We created a non-stimulatory version of the oligo CpG2216 by inverting the stimulatory CpG motifs to GpC, to generate GpC2216. As shown in Figure 6D, the stimulatory CpG2216 induced Interleukin-6 (IL-6) production in BMDCs and this was inhibited by 10 μ M AT791. However, when an excess of the non-stimulatory GpC2216 was also added, induction of IL-6 was restored. GpC2216 itself, either alone or in the presence of AT791, did not stimulate IL-6 production (Fig. 6D). These results are consistent with the idea that suppression of TLR9 by AT791 involves an interaction of the compound with DNA.

Analysis of compound-DNA interaction

We analyzed compound-DNA interaction using fluorescence spectrometry and equilibrium dialysis. AT791 and E6446 are intrinsically fluorescent and have similar fluorescence spectra of 312nm peak excitation and 381nm peak emission (Supplemental Figure 5). Starting with 200nM AT791 or E6446, we added increasing amounts of CpG2006 or SL4 RNA and observed that compound fluorescence decreased in a quantitative and saturable manner (Fig. 6C). The same experiment using 2-aminopurine, a compound that has a similar fluorescence spectrum to AT791 and E6446, resulted in no change in fluorescence (Fig. 6C).

MOL #89821

Changes in compound fluorescence as a function of nucleic acid concentration showed an almost perfect fit to a one-site binding curve ($R^2 > 99\%$) with K_d s in the 1 ~ 4 μM range, similar to the IC_{50} s obtained in the *in vitro* DNA – TLR9 interaction assay (Fig. 6A). We confirmed these results using an equilibrium dialysis method with an 8 kDa cutoff membrane. AT791 (200nM) was added to both chambers and various concentrations of DNA (3X-CpG2006; 22kDa) were added to one chamber. After overnight incubation, compound concentrations in each chamber were quantitated by mass spectrometry. We obtained an almost perfect fit to a one-site binding curve ($R^2 = 99.6\%$) and a K_d of ~ 3.4 μM (Supplemental Figure 6). In both the fluorescence quenching and equilibrium dialysis assays, DNA and RNA were in large molar excess over compound, thus the K_d s here represent the binding of one drug molecule per oligonucleotide, although when higher concentrations of AT791 were mixed with CpG2006 and injected directly into a mass spectrometer, we could detect the binding of multiple drug molecules to the oligonucleotides (data not shown). By the fluorescence spectroscopy method we also found that the affinities of AT791 for the *in vitro* decoy oligo CpG1417 was 16 μM +/- 3.2 μM and that for the *in vivo* decoy oligo GpC2216 was 0.8 μM +/- 0.1 μM (data not shown).

To further test the idea that small molecule interaction with nucleic acids might be able to inhibit TLR signaling, we tested whether known DNA-binding molecules could inhibit TLR7 and 9. We found that the dimeric cyamine DNA dye YOYO-1 could suppress DNA- or RNA-induced signaling in a concentration-dependent manner (Fig. 3). Although YOYO-1 is relatively cell-impermeant, we observed that at high concentrations YOYO-1 fluorescence appeared in a punctate pattern in the cytoplasm of RAW 264.7 cells (data not shown). As seen for AT791 and E6446, YOYO-1 inhibits DNA- and RNA-induced signaling, but not imidazoquinoline- or LPS-induced signaling. Similar to these results, Kuznik et al (2011)

have also recently observed that TLR9 activation by stimulatory DNA can be inhibited by the DNA-binding dyes Hoechst 34580 and propidium iodide.

Compound localization and accumulation

The concentrations of AT791 and E6446 required to bind to nucleic acids and inhibit DNA-TLR9 interaction *in vitro* are at least 100x greater than the concentrations required to inhibit TLR7 or 9 signaling in cells, suggesting these compounds might accumulate in cells. Direct visualization of AT791 and E6446 in cells by conventional fluorescence microscopy is hampered by their low excitation wavelength (~310 nm), which does not transmit well through ordinary microscope glass. We used two methods to circumvent this limitation: two-photon microscopy, which uses 2x the normal wavelength to excite the fluorescent molecule, and high-intensity off-peak excitation with a 351 nm UV laser. When HEK cells were incubated with 1 μ M AT791 and visualized with two-photon excitation, compound fluorescence appeared within a few minutes as a punctate pattern in the cell cytoplasm (Fig. 7), and overlapped that of the lysosomal marker Lamp-1 (Supplemental Figure 7A). We observed a similar cytoplasmic punctate pattern in C33A cells incubated with 1 μ M AT791 and visualized by high-intensity 351 nm excitation (Supplemental Figure 7B). Comparing the intracellular fluorescence intensities to a calibration curve generated by spotting different concentrations of AT791 on a slide, we could estimate intra-vesicle AT791 concentration to be in the 1 to 2 mM range (Supplemental Figure 7B). These results indicate that AT791 and E6446 can accumulate several orders of magnitude inside lysosomes.

AT791 and E6446 are typical of “lysosomotropic” compounds in that they are lipophilic and contain weak base amines. At neutral pH, such compounds are non-polar and can penetrate lipid membranes, but within low pH vesicles they become protonated and are trapped

MOL #89821

(DeDuve et al., 1974). Capillary electrophoresis showed that AT791 has pK_as of 7.9 and 6.1, and E6446 has pK_as of 8.6 and 6.5, indicating they would be more highly protonated in endolysosomal compartments compared to cytoplasm. We examined the pH-dependent lipid permeability of these compounds using a Parallel Artificial Membrane Assay (PAMPA) assay, which consists of two aqueous chambers containing pH 7.4, 6.5 or 5.5 buffers, separated by a hydrophobic layer of *L*- α -phosphatidylcholine. In an overnight assay, the compounds readily penetrated the *L*- α -phosphatidylcholine layer at pH 7.4, but were almost completely non-permeant at or below pH 6.5 (Table II). We next established a pH gradient across the PAMPA membrane, adding pH 5.5 buffer to one chamber and pH 7.4 buffer to the other. Pilot experiments showed that this pH gradient can be maintained at least overnight. When 5 mM AT791 or E6446 were added to both chambers, we observed a steady re-distribution of the compounds into the pH 5.5 compartment over 8 hours (Fig. 8). Thus the ability of these compounds to accumulate in low-pH compartments is an intrinsic chemical property. We observed that accumulation of these compounds in living cells occurred within minutes (Fig. 7). This rapid accumulation is presumably due to the very high surface-to-volume ratio of intracellular vesicles.

If accumulation of these compounds in endolysosomal compartments is necessary for their activity, they should be ineffective at inhibiting TLR7 or 9 localized elsewhere in the cell. We tested this idea using a receptor fusion between the TLR9 ectodomain and the TLR4 cytoplasmic domain (9N4C), which localizes to the cell surface and signals in response to stimulatory DNA (Barton et al., 2006). HEK cells expressing either full-length TLR9 or the 9N4C chimera were stimulated with CpG2006 oligonucleotides. We saw the expected inhibition of reporter activity by AT791 (1 μ M) in cells expressing full-length TLR9, but not in cells expressing 9N4C (Fig 9). Similar results were obtained with E6446 (data not shown).

In vivo efficacy

AT791 and E6446 are orally bioavailable (AT791, 41%; E6446, 20%) and have high volumes of distribution in mice (AT791, 12.8 L/kg; E6446, 95.9 L/kg). To test their activity *in vivo*, mice were orally dosed with 20mg/kg of AT791 or E6446, and 18 hours later were challenged with 60 μ g CpG1668 oligonucleotide injected subcutaneously. CpG1668-induced IL-6 production was inhibited approx. 50% by AT791 and almost completely by E6446 (Fig 10A). We took the more active compound, E6446, and tested it in a MRL/lpr mouse SLE model. MRL/lpr females were dosed orally with 20 or 60 mg/kg of E6446 per day, five days a week, starting at one month of age. Anti-nuclear antibody (ANA) development was followed by immunofluorescence staining of Hep2 cells with the mouse sera and scoring for degrees of severity. Sera from untreated mice developed ANA reactivity gradually over the observation period, culminating in 11 of the 12 animals showing some degree of ANA-positivity by 18 weeks (Fig. 10B). In contrast, development of ANA was suppressed in a dose-dependent manner in animals treated with 20 mg/kg and at 60 mg/kg E6446. Examination of anti-double stranded DNA (dsDNA) titers gave a similar result, with E6446 partially suppressing the development of circulating anti-dsDNA antibodies in a dose-dependent manner (Fig. 10C). A control immunosuppressing agent cyclophosphamide (Cytosan) effectively blocked autoantibody development (Fig. 10D). Although E6446 suppressed ANA development, we saw no suppression of proteinuria (data not shown).

Inhibition of TLR7 and 9 by antimalarials

Hydroxychloroquine (Plaquenil) is prescribed for the treatment of lupus, and both hydroxychloroquine and its analog chloroquine inhibit TLR7 and 9 signaling (MacFarlane & Manzel, 1998), results that we confirmed in Figure 3 (right panels) and Table I. We noticed a

MOL #89821

number of similarities between the antimalarials and our compounds. Chloroquine interacts with double-stranded DNA (Cohen & Yielding, 1965) and accumulates in acidic compartments in cells (French et al., 1987). The antimalarials also exhibit a similar pattern of inhibition to AT791 and E6446: they more potently antagonize TLR7 signaling induced by RNA than the imidazoquinolines CL-097 or R-848 (Fig. 3, right panels and Table I). We therefore asked if these compounds might utilize a mechanism of action similar to that of AT791 and E6446 to inhibit TLR7 and 9 signaling. We observed that the intrinsic fluorescence of both antimalarials is quenched in the presence of CpG2006, and the data showed an excellent fit to a one-site binding curve with virtually identical Kds of $57\mu\text{M} \pm 5\mu\text{M}$ for both compounds ($R^2 > 99\%$) (Supplemental Figure 8). Given that the antimalarials have IC_{50} values in cell-based assays in the $1 \sim 5\mu\text{M}$ range, they would need to accumulate inside cells approximately 10 ~ 20-fold in order to achieve concentrations sufficient to interact with nucleic acids. In the PAMPA assay (Table II), both hydroxychloroquine and chloroquine were permeant at physiological pH, but non-permeant at pH 6.5 and below. Finally, neither hydroxychloroquine nor chloroquine produced any detectable change in intracellular pH at $5\mu\text{M}$ (Fig. 5), similar to the observations of Manzel et al (1999) and Kuznik et al. (2011). These data suggest that chloroquine and hydroxychloroquine may inhibit TLR7 and 9 signaling by accumulating inside cells and binding to nucleic acids, similar to AT791 and E6446, and not by modulation of pH. A similar conclusion was recently reported by Kuznik et al (2011) based on their studies of the antimalarials chloroquine and quinacrine.

Discussion

These data indicate that the ability of AT791 and E6446 to antagonize TLR7 and TLR9 signaling depends on two intrinsic properties: (1) their affinity for DNA, and (2)

MOL #89821

accumulation in intracellular acidic compartments. It should be noted that the Kds for the interaction of these compounds with DNA is in the μM range, which is relatively weak. At the concentrations used to antagonize TLR7 and 9 in cells (10 ~ 50nM), there should be no significant interaction with DNA except in the intracellular vesicles where the compounds are concentrated. This localized action of the compounds may be beneficial, as it would limit potential off-target liabilities such as mutagenicity.

How does interaction of AT791 or E6446 with DNA inhibit TLR7 or TLR9 activation? As we observed *in vitro*, these compounds can interfere with DNA-TLR9 interaction. However, we found one analog of AT791 that enhanced DNA-TLR9 interaction *in vitro*, yet inhibited TLR9 activation in cell-based assays (data not shown), suggesting the involvement of other mechanisms of inhibition. DNA binding alone is not sufficient to activate TLR9, and certain DNA conformations and sequences, such as CpG motifs, are required to trigger a signaling event that is accompanied by a conformational change in TLR9 (Latz et al., 2007). Therefore, another way in which compounds such as AT791 and E6446 could inhibit TLR7 and 9 signaling is to render nucleic acids non-stimulatory by masking stimulatory sequences and/or altering their conformation.

AT791 and E6446 share several characteristics with a number of clinically approved lysosomotropic drugs such as haloperidol, levomepromazine and amantadine. All of these drugs are lipophilic, contain weak bases, exhibit high volumes of distribution *in vivo* and have long elimination half-lives. The accumulation of weak bases inside acidic vesicles has the potential to neutralize vesicle pH, and indeed chloroquine, methylamine and ammonium chloride are commonly used as biological reagents for this purpose. However, modulation of pH does not appear to explain inhibition of TLR7 and 9 signaling either by

MOL #89821

AT791, E6446 or by the antimalarials chloroquine or hydroxychloroquine. First, we failed to see any significant effect of these compounds on endosome / lysosome pH using pH-sensitive fluorescent dyes. Strictly speaking, we do not know how the distribution of the TLR7 and 9 receptors overlaps with the dextran-containing, bright vesicles that we were able to visualize and quantitate. Furthermore, at concentrations higher than those used in the present study, AT791, E6446, chloroquine and hydroxychloroquine can all alter the fluorescence of both pH-sensitive and pH-insensitive fluorescent dyes, possibly due to direct molecular interactions between these molecules, e.g. hydrophobic ring stacking.

A stronger case is made by the distinct patterns of TLR7 antagonism caused by AT791, E6446, the antimalarials, known pH modulators and the DNA binding dye YOYO-1. These patterns of antagonism fall into two distinct groups: the known pH modulators antagonize TLR 7 activation by both RNA and imidazoquinoline ligands more or less equally, whereas AT791, E6446, the antimalarials, and YOYO-1 are highly selective for RNA versus the imidazoquinolines. Kuznik et al. (2011) also noted the selective antagonism of nucleic acid ligands by chloroquine, quinacrine and the DNA-binding dyes propidium iodide and Hoechst 34580. However, at higher concentrations, AT791, E6446, chloroquine and hydroxychloroquine can antagonize TLR7 induction by imidazoquinolines, probably because the accumulation of these weak bases is now sufficient to modulate endosomal pH. The window of selectivity between antagonizing RNA versus imidazoquinoline induction of TLR7 is 6~8-fold for chloroquine or hydroxychloroquine, and 20~40-fold for AT791 and E6446. This greater window of selectivity for AT791 and E6446 is presumably due to their higher affinity for nucleic acids. In SLE patients treated with daily doses of 200 ~ 400mg hydroxychloroquine, steady-state concentration of drug in the plasma has been reported to be in the range of 200 ~ 1000 ng/ml, or 0.4 ~ 2.0 μ M (Tett et al., 1989). This is the

MOL #89821

concentration range at which hydroxychloroquine can inhibit TLR7 and 9 in cell culture, but below the concentration required to alter endosomal pH. Indeed, hydroxychloroquine has been reported to be toxic in humans at a plasma concentration of 29 μM (Jordan et al, 1999). Thus, AT791 and E6446 may be considered more optimized versions of Plaquenil, functioning via the same mechanism of action to suppress TLR7 and 9 signaling, but providing a greater margin of selectivity.

In the spontaneous MRL/lpr mouse model of SLE, E6446 suppressed the development of anti-nuclear and anti-DNA antibodies, but not the development of glomerular nephritis. These results resemble those obtained with a TLR9^{-/-} MRL/lpr mouse (Christensen et al., 2005). However, the role of TLR9 and TLR7 in the development of murine lupus is complex and may vary with the mouse model and experimental conditions. It has been reported that in some models TLR9 knockout can exacerbate lupus nephritis, that ablation of TLR7 is more effective at ameliorating disease, and that TLR9 modulates TLR7 activity (Wu et al., 2006, Christensen et al, 2006, Nickerson et al., 2010). A study using an oligonucleotide dual antagonist of TLR7 and TLR9 also reported efficacy in murine lupus models, showing reductions in anti-dsDNA titers in NZBxNZW and MRL models, and some positive impact on proteinuria and mortality (Barrat et al., 2007, Pawar et al., 2007).

Recently, Franklin et al (2011) have shown that E6446 is effective in preventing hyper-inflammation and lethality caused by the parasite *Plasmodium berghei* in a mouse model of cerebral malaria. Thus these compounds show efficacy in two very different animal models of disease driven in part by TLR activation. Taken together with the known efficacy of hydroxychloroquine and other antimalarials in human disease, the data presented here suggest a common mechanism of action for two structurally diverse families of endosomal

MOL #89821

TLR inhibitors.

Acknowledgments

The assistance of the animal facility staff is gratefully acknowledged. All authors except E. Latz, and T. Mempel are or were employees of Eisai at the time this work was performed. Dr. Latz has participated in a previous sponsored research agreement with Eisai Research Institute. We thank Dr. Greg Barton (UC, Berkeley) for the HEK cell line expressing 9N4C, and Douglas Golenbock, Seiichi Kobayashi, Geoffrey Hird, Jiping Liu, Matthew Mackey and Lynn Hawkins for their helpful contributions and discussions. Portions of these results were presented at the meeting “Toll 2008: Recent Advances in Pattern Recognition” (Portugal, 2008).

Authorship contributions

Participated in research design: Lamphier, Zheng, Latz, Spyvee, Hansen, Zhao, Shen, Chow, Yu, Gusovsky, Ishizaka
Conducted experiments: Lamphier, Genest, Latz, Hansen, Rose, Yang, Zhao, Shen, C. Liu, D. Liu, Mempel, Rowbottom, Twine,
Contributed new reagents or analytic tools: Zheng, Latz, Shaffer, Shen, Mempel,
Performed data analysis: Lamphier, Latz, Hansen, Rose, Yang, Zhao, D. Liu, Mempel, Rowbottom, Twine, Yu, Ishizaka
Wrote or contributed to the writing of the manuscript: Lamphier, Mempel, D. Liu, Twine, Ishizaka

References

- Barbalat R, Ewald SE, Mouchess ML, and Barton GM. (2011) Nucleic acid recognition by the innate immune system. *Annu Rev Immunol.* **29**:185-214
- Bamboatz ZM, Balachandran VP, Ocui LM, Obaid H, Plitas G, DeMatteo RP. (2010) Toll-like receptor 9 inhibition confers protection from liver ischemia-reperfusion injury. *Hepatology.* **51**:621-632.
- Barrat, F. J., T. Meeker, J. H. Chan, C. Guiducci, and R. L. Coffman. (2007) Treatment of lupus-prone mice with a dual inhibitor of TLR7 and TLR9 leads to reduction of autoantibody production and amelioration of disease symptoms. *Eur. J. Immunol.* **37**:3582-3586.
- Barton GM, Kagan JC, and Medzhitov R. (2006) Intracellular localization of Toll-like receptor 9 prevents recognition of self DNA but facilitates access to viral DNA. *Nat Immunol* **7**:49–56
- Calcaterra C, Sfondrini L, Rossini A, Sommariva M, Rumio C, Ménard S, Balsari A.(2008) Critical role of TLR9 in acute graft-versus-host disease. *J Immunol.* **181**:6132-6139.
- Christensen, S.R., M. Kashgarian, L. Alexopoulou, R.A. Flavell, S. Akira, and M.J. Shlomchik. (2005). Toll-like receptor 9 controls anti-DNA autoantibody production in murine lupus. *J.Exp. Med.* **202**:321-331.
- Christensen, S.R., J. Shupe, K. Nickerson, M. Kashgarian, R.A. Flavell, and M.J. Shlomchik. (2006) Toll-like receptor 7 and TLR9 dictate autoantibody specificity and have opposing inflammatory and regulatory roles in a murine model of lupus. *Immunity* **25**:417-428.
- Cohen SN and Yielding KL (1965) Spectrophotometric Studies of the Interaction of Chloroquine with Deoxyribonucleic Acid. *J. Biol. Chem.* **240**: 3123-3131.
- De Duve C, De Barse T, Poole B, Trouet A, Tulkens P, Van Hoof F. (1974) Commentary. Lysosomotropic agents. *Biochem Pharm.* **23**:2495–2531.
- Franklin BS, Ishizaka ST, Lamphier M, Gusovsky F, Hansen H, Rose J, Zheng W, Ataíde MA, de Oliveira RB, Golenbock DT, Gazzinelli RT. (2011) Therapeutic targeting of nucleic acid-sensing Toll-like receptors prevents experimental cerebral malaria. *Proc Natl Acad Sci U S A.* **108** :3689-3694.
- French, JK, Hurst, N P, O'Donnell, M L, and Betts, W H (1987) Uptake of chloroquine and hydroxychloroquine by human blood leucocytes in vitro: relation to cellular concentrations during antirheumatic therapy. *Ann Rheum Dis.* **46**: 42–45.
- Hemmi, H., T. Kaisho, O. Takeuchi, S. Sato, H. Sanjo, K. Hoshino, T. Horiuchi, H. Tomizawa, K. Takeda, and S. Akira. (2002) Small anti-viral compounds activate immune cells via the TLR7 MyD88-dependent signaling pathway. *Nat. Immunol.* **3**:196-200

- Hoque R, Sohail M, Malik A, Sarwar S, Luo Y, Shah A, Barrat F, Flavell R, Gorelick F, Husain S, Mehal W. (2011) TLR9 and the NLRP3 inflammasome link acinar cell death with inflammation in acute pancreatitis. *Gastroenterology* **141**:358-369.
- Itagaki K, Adibnia Y, Sun S, Zhao C, Sursal T, Chen Y, Junger W, Hauser CJ. (2011) Bacterial DNA induces pulmonary damage via TLR-9 through cross-talk with neutrophils. *Shock* **36**:548-552.
- Ishizaka, S. (2008) Development and *in vivo* assessment of TLR9 inhibitors. Presentation at *Toll 2008: Recent Advances in Pattern Recognition* (Portugal, 2008).
- Jordan, P., Brookes, J. G, Nikolic, G., Le Couteur, D. G., and Le Couteur, D. (1999) Hydroxychloroquine Overdose: Toxicokinetics and Management. *Clin Tox* **37**: 861-864.
- Kimball A, Krueger J, Sullivan T, Arbeit R. (2013) IMO-3100, an antagonist of TLR7 and TLR9, demonstrates clinical activity in psoriasis patients with 4 weeks of treatment in a phase 2a trial. Abstract 158, International Investigative Dermatology, May 8-11, 2013.
- Klaschik S., I. Gursel, and D.M. Klinman. (2007) CpG-mediated changes in gene expression in murine spleen cells identified by microarray analysis. *Mol. Immunol.* **44**:1095-1104.
- Kuznik A, Bencina M, Svajger U, Jeras M, Rozman B, Jerala R. (2011). Mechanism of endosomal TLR inhibition by antimalarial drugs and imidazoquinolines. *J Immunol.* **186**:4794-4804.
- Latz, E., A. Schoenemeyer, A. Visitin, K.A. Fitzgerald, B.G. Monks, C.F. Knetter, E. Lien, N.J. Nilsen, T. Espevik and D.T. Golenbock. (2004) TLR9 signals after translocating from the ER to CpG DNA in the lysosome. *Nat. Immunol.* **5**:190-198.
- Latz, E., A. Verma, A. Visintin, M. Gong, C.M. Sirois , D.C. Klein, B.G. Monks, C.J. McKnight, M.S. Lamphier, W.P. Duprex, T. Espevik, and D.T. Golenbock. (2007) Ligand-induced conformational changes allosterically activate Toll-like receptor 9. *Nat. Immunol.* **8**:772-779.
- Leadbetter EA, Rifkin IR, Hohlbaum AM, Beaudette BC, Shlomchik MJ, Marshak-Rothstein A. (2002) Chromatin-IgG complexes activate B cells by dual engagement of IgM and Toll-like receptors. *Nature* **416**:603–607.
- MacFarlane, D.E., and L. Manzel. (1998). Antagonism of immunostimulatory CpG-oligodeoxynucleotides by quinacrine, chloroquine, and structurally related compounds. *J. Immunol.* **160**:1122-1131.
- Manzel L., L. Strekowski, F. M. Ismail, J. C. Smith, D. E. Macfarlane. Antagonism of immunostimulatory CpG oligodeoxynucleotides by 4-aminoquinolines and other weak bases: mechanistic studies. (1999). *J Pharmacol Exp Ther.* **291**:1337-1347.
- Marshak-Rothstein A. (2006) Toll-like receptors in systemic autoimmune disease. *Nat Rev Immunol.* **6**:823-835.

MOL #89821

Means T.K., E. Latz, F. Hayashi, M.R. Murali, D.T. Golenbock, and A.D. Luster. (2005) Human lupus autoantibody-DNA complexes activate DCs through cooperation of CD32 and TLR9. *J. Clin. Invest.* **115**:407-417.

Nickerson KM, Christensen SR, Shupe J, Kashgarian M, Kim D, Elkon K, Shlomchik MJ. (2010) TLR9 regulates TLR7- and MyD88-dependent autoantibody production and disease in a murine model of lupus. *J Immunol.* **184**:1840-1848.

Pawar, R.D., A. Ramanjaneyulu, O.P. Kulkarni, M. Lech, S. Segerer, and H.-J. Anders. (2007) Inhibition of Toll-like receptor-7 (TLR-7) or TLR-7 plus TLR-9 attenuates glomerulonephritis and lung injury in experimental lupus. *J. Am. Soc. Nephrol.* **18**:1721-1731.

Sasai M, Yamamoto M. (2013) Pathogen recognition receptors: ligands and signaling pathways by toll-like receptors. *Int Rev Immunol.* **32**:116-133.

Tett, S. E., Cutler, D. J, Day, R O and Brown, K F. (1989) Bioavailability of hydroxychloroquine tablets in healthy volunteers. *Br J Clin Pharmacol.* **27**: 771-779.

Vallin, H., A. Perers, G.V.Alm, and L. Rönnblom. (1999) Anti-double-stranded DNA antibodies and immunostimulatory plasmid DNA in combination mimic the endogenous IFN- α inducer in systemic lupus erythematosus. *J. Immunol.* **163**:6306-6313.

Wohnsland, F. and Faller, B. (2001) High-throughput Permeability pH Profile and High-throughput Alkane/Water Log P With Artificial Membranes, *J. Med. Chem.*, **44**:923-930.

Wu, X. and S.L. Peng. (2006) Toll-like receptor 9 signaling protects against murine lupus. *Arthritis Rheum.* **54**:336-342.

Legends for Figures

Figure 1. AT791 and E6446 structures and activities. A, Molecular structures. B, Suppression of Interleukin-6 production by mouse bone marrow-derived dendritic cells. Cells were treated with various concentrations of AT791 or E6446 and then stimulated overnight with the indicated agonists.

Figure 2. Interleukin-6 production by DNA-antibody complexes is suppressed by AT791. A, Anti-DNA antibodies and DNA synergistically stimulate production of IL-6 in mouse bone marrow-derived dendritic cells. Anti-biotin antibody was used as a control. Data indicates that an optimal stoichiometry is required for efficient induction. B, Stimulation by DNA-antibody complexes is suppressed by AT791.

Figure 3. Selectivity of TLR inhibitors. RAW 264.7 cells containing an NF- κ B:luciferase reporter were stimulated with optimal concentrations (approx. EC₉₀) of CpG1668 (DNA), RNA40 (RNA), CL-097 or LPS in the presence of a range of concentrations of the indicated inhibitors. After overnight incubation, luciferase activities were measured.

Figure 4. Uptake of OligoDNA – Phycoerythrin complexes by RAW 264.7 cells. DNA-phycoerythrin complexes are taken up by RAW264.7 cells within 30 minutes when incubated at 37 °C, but remain on cell surface when incubated at 4 °C. AT791 and E6446, even at a relatively high concentration (1 μ M), have no obvious effect on complex uptake or localization

Figure 5. Effects of compounds on intracellular pH. Compound concentrations approximate the IC₉₀ for inhibition of TLR9 stimulation in RAW264.7 cells. Cells were pre-loaded with dextrans conjugated to the pH-sensitive dyes FITC and pHrodo and fluorescence in intracellular vesicles was quantitated by confocal microscopy. Bafilomycin (BAF), methylamine (MA) and Monensin (MN) cause a significant increase in the FITC:pHrodo, indicating an increase in pH. In contrast, concentrations of AT791, E6446, chloroquine (CHL) or hydroxychloroquine (HCQ) sufficient to suppress TLR9 stimulation do not cause an increase in pH.

Figure 6. In vitro and in vivo characterization of AT791 and E6446. A. AT791 and E6446 suppress TLR9 – DNA interaction in vitro, with an IC₅₀ in the 1 to 10 μ M range. B. Inhibition of TLR9-DNA interaction by AT791 can be relieved in the presence of an excess of a short competitor oligonucleotide CpG1417, which does not interact with TLR9. C. Addition of CpG2006 DNA (circles) or SL4 RNA (crosses) causes a quantitative change in the intrinsic fluorescence of AT791 and E6446, but not of a control compound 2-aminopurine. Fit to one-site binding curve (Graphpad Prism) gives K_ds in the 2 to 5 μ M range (n=3), with R² goodness to fit >99%. D. Excess non-stimulatory oligoGpC2216 can relieve suppression of IL-6 production by AT791 in living cells (BMDCs).

Figure 7. Two-photon imaging of AT791 in living HEK cells. AT791 (1 μ M) was added to cultures of HEK cells and imaged 15 minutes later by two-photon microscopy. AT791 (red)

MOL #89821

appears in a punctate pattern within the cytoplasm. Smad2-GFP is constitutively expressed and marks the cytoplasm.

Figure 8. pH partitioning of AT791 and E6446. AT791 and E6446 (5 μ M) were evenly distributed between chambers containing two different pH buffers and separated by a hydrophobic barrier. Over the next 8 hours, compounds re-distributed to the low pH compartment.

Figure 9: AT791 does not inhibit cell surface-expressed TLR9. A chimera consisting of the TLR4 cytoplasmic and transmembrane regions and the TLR9 ectodomain is expressed on the cell surface and induces NF- κ B signaling in response to CpG2006 DNA. Whereas AT791 inhibits activation by the full-length, intracellular TLR9 (left panel), it has no effect on activation of the cell-surface expressed chimera (right panel).

Figure 10: In vivo efficacy of AT791. A. short-term induction of serum interleukin-6 in mice by CpG1668 DNA is effectively suppressed by pre-treatment with 20 mg/kg AT791 or E6446. Data are representative of two experiments. B. Anti-nuclear antibody (ANA) titers in 18-week old MRL/lpr mice are suppressed in a dose-dependent manner by E6446, given starting at week 5. Data representative of two experiments C. Development of anti-dsDNA antibodies in MRL-lpr mice is also suppressed by E6446. “pre” are serum samples taken before dosing at 5 weeks of age, “post” are samples taken after 7 weeks of E6446 dosing. Post-treatment samples are compared with vehicle control by one-way ANOVA with Newman-Keuls post-test. ** differs from vehicle with $p < 0.01$, * differs from vehicle with $p < 0.05$. Data representative of two experiments. D) Controls for experiments shown in panel C. Hydroxychloroquine (60 mg/kg, 5x per week) had no impact on anti-dsDNA, while cytoxan (50mg/kg, 1x per 10 days) caused a statistically significant suppression in titers. Statistical analysis as in C.

Table 1: Potency of small molecule inhibitors in engineered and primary cells

Responding Cells	Stimulus	Readout	IC ₅₀ (μM)		
			AT791	E6446	Hydroxy-chloroquine
HEK-TLR9	CpG2006	NF-κB – luc	0.04	0.01	0.08
HEK-TLR7	R848	NF-κB – luc	3.33	1.78	2.78
HEK-TLR4	LPS	NF-κB – luc	>10	10.58	>30
Mouse spleen	CpG1668	IL-6	0.04	0.02	3.1
	R848	IL-6	8.0	4.9	>10
	LPS	IL-6	8.9	N.D.	>10
Human PBMC	CpG2216	IL-6	0.21	0.23	1.2
		α-interferon	0.41	0.09	1.2
	CpG2006	IL-6	N.D.	0.28	N.D.

Luciferase reporter lines or primary mouse or human cells were stimulated overnight and activation assessed by NF-κB-luciferase reporter or cytokine ELISA as described in Materials and Methods. Results are the mean of 2 to 5 separate determinations. N.D. = not determined.

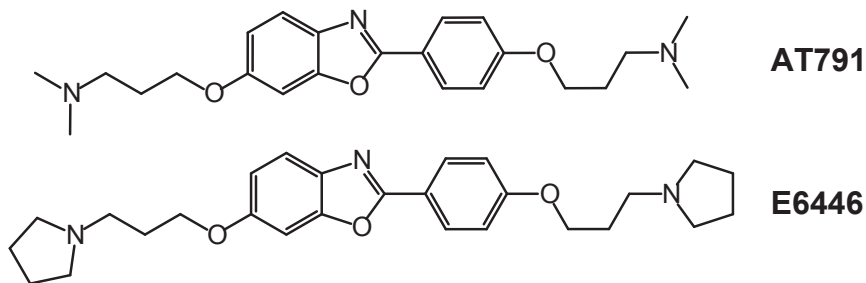
Table 2: Effect of pH on permeability of compounds

	Permeability (x 10 ⁻⁶ cm/s)		
	pH7.4	pH6.5	pH5.5
AT791	58.5	0.1	0.2
E6446	67.4	0.3	0.4
Hydroxychloroquine	1.7	0.2	0.0
Chloroquine	19.5	3.7	1.4

10 μ M AT791, 10 μ M E6446, 40 μ M hydroxychloroquine, or 40 μ M chloroquine in were assayed in a Parallel Artificial Membrane Permeation Assay, as described in Materials and Methods. Data represent the average of three replicates. Permeability was calculated according to Wohnsland & Faller (2001).

Figure 1

A



B

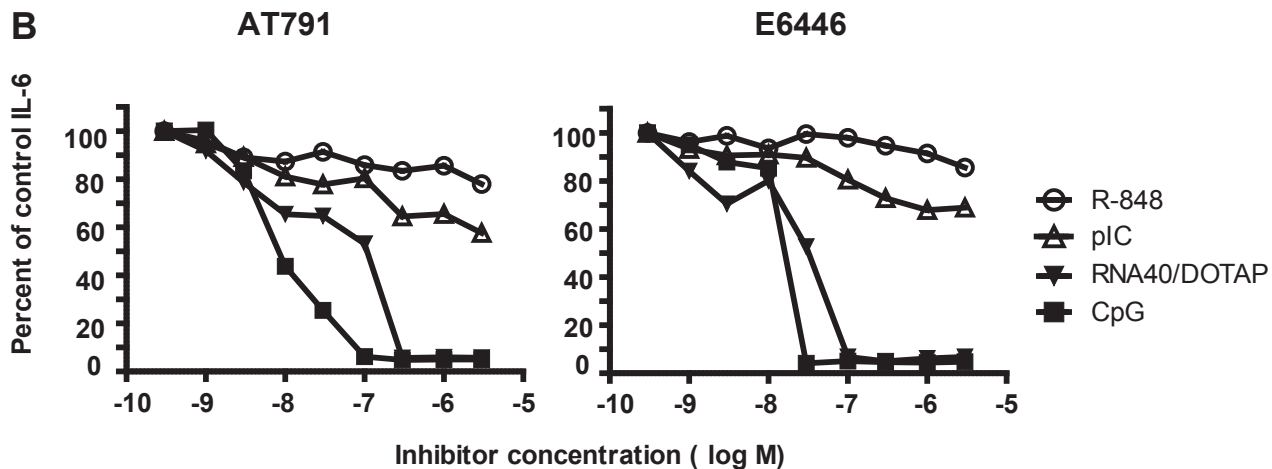
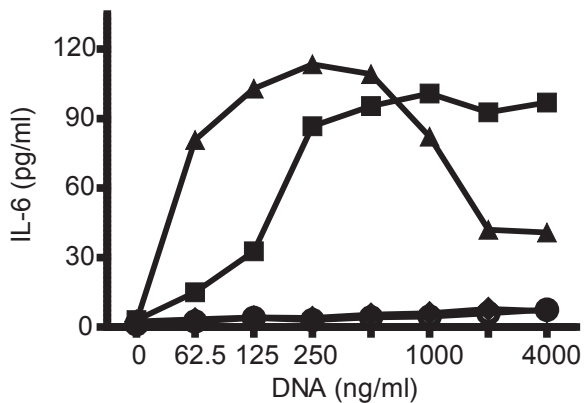


Figure 2

A



Antibody:

- Anti-DNA 1:25
- ◆ Anti-biotin 1:25
- ▲ Anti-DNA 1:200
- None

B

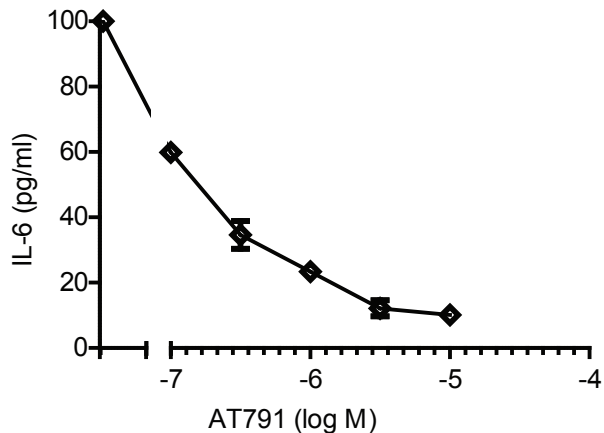


Figure 3.

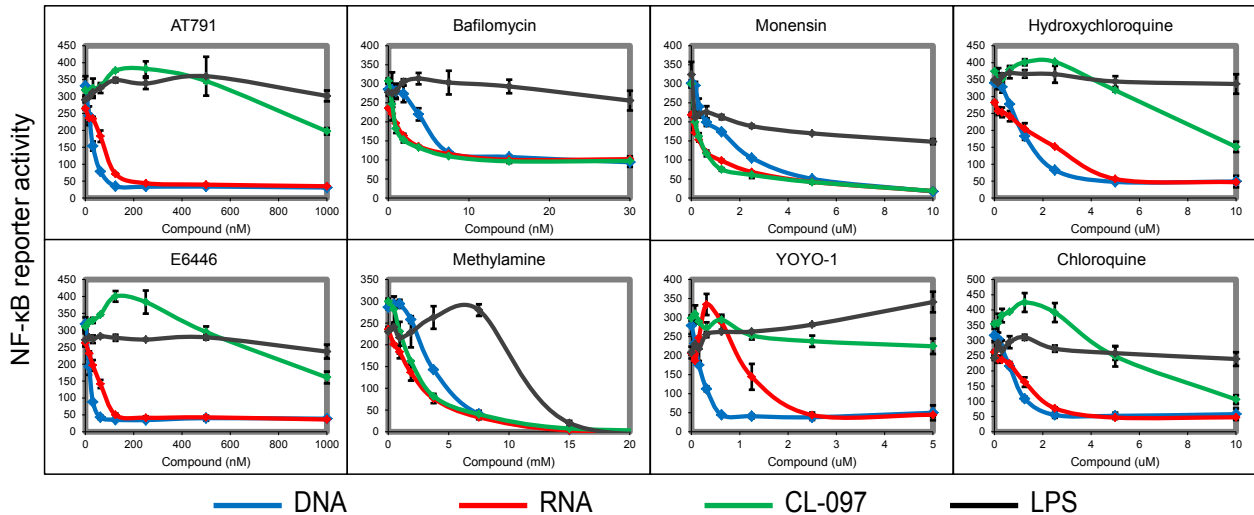
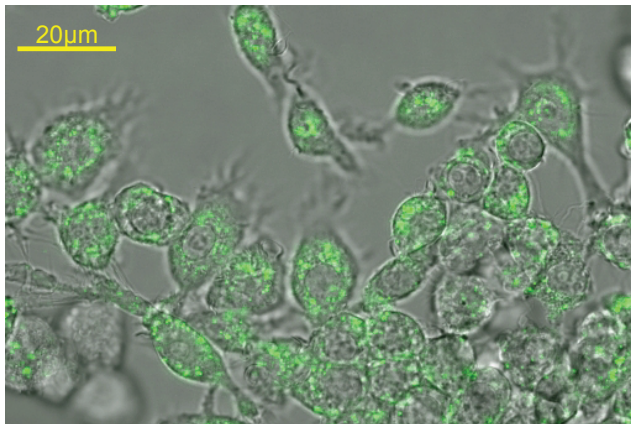
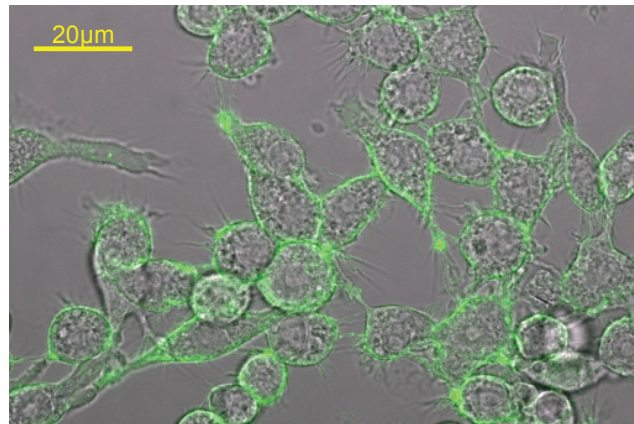


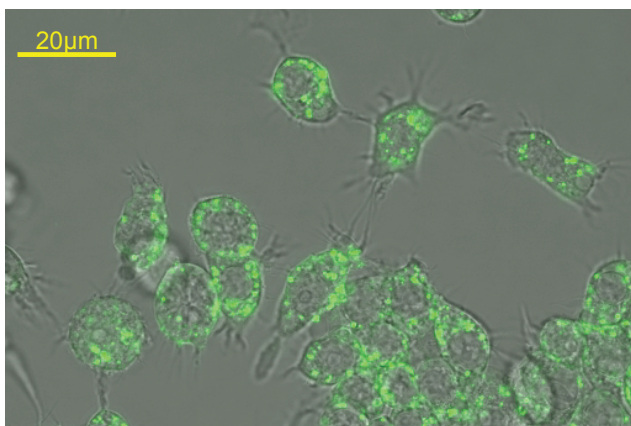
Figure 4



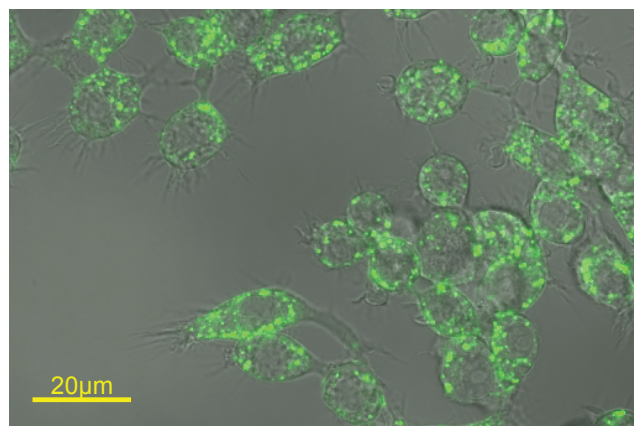
37°C



4°C



37°C - 1 µM E6446



37°C - 1 µM E6446

Figure 5

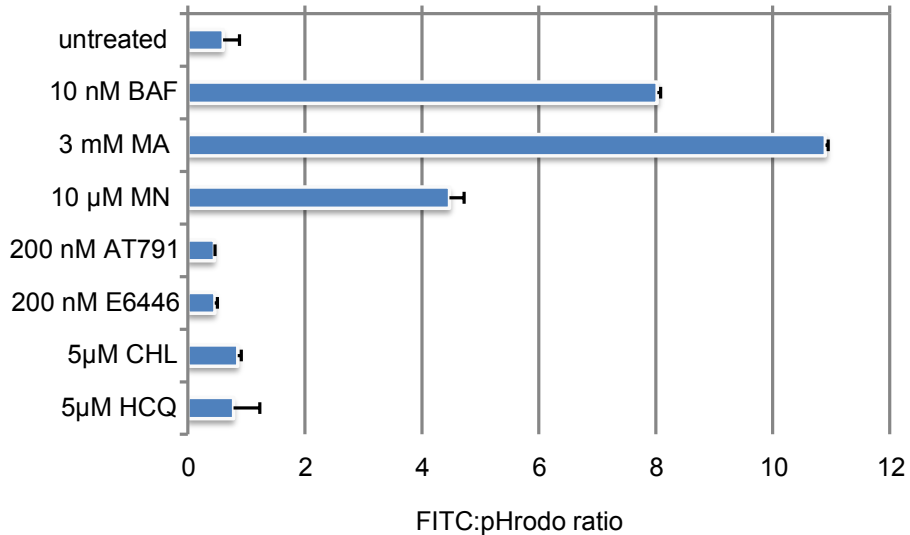
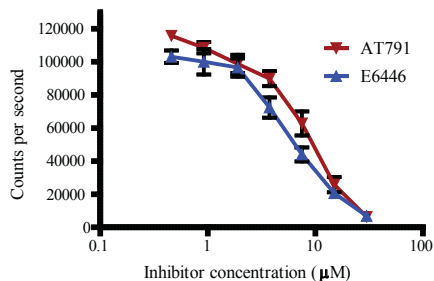
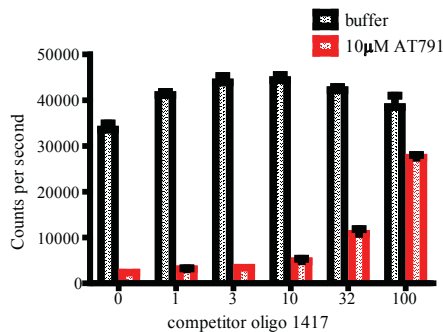


Figure 6

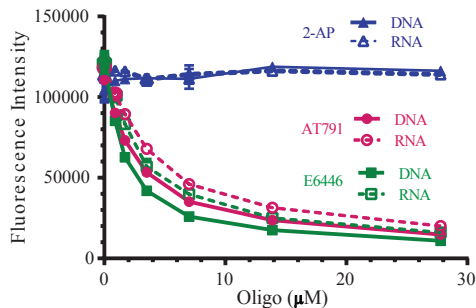
A



B



C



	DNA		RNA		Kds (μM)
AT791	2.5	(± 0.1)	3.6	(± 0.4)	
E6446	1.4	(± 0.2)	2.6	(± 0.3)	

D

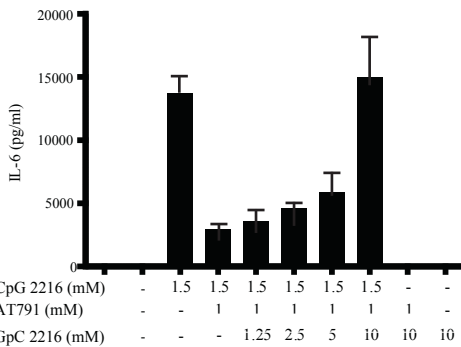
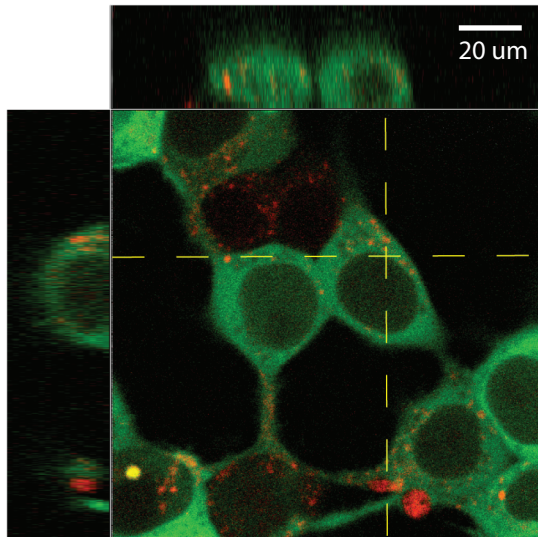
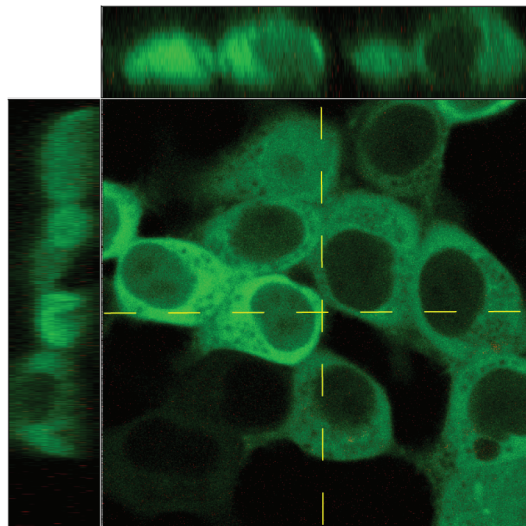


Figure 7



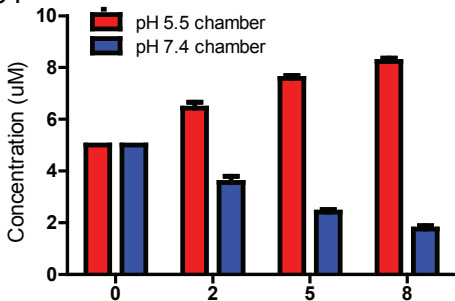
1 μ M AT791 Smad2-EGFP



(control) DMSO Smad2-EGFP

Figure 8

AT791



E6446

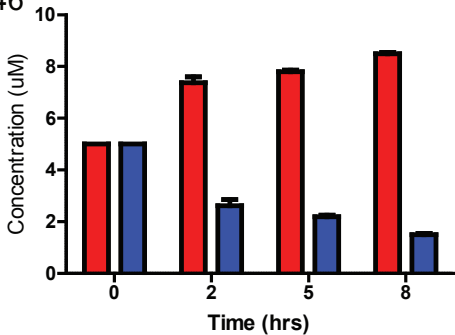


Figure 9

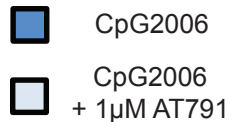
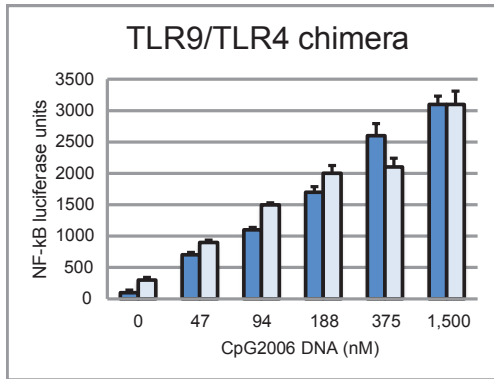
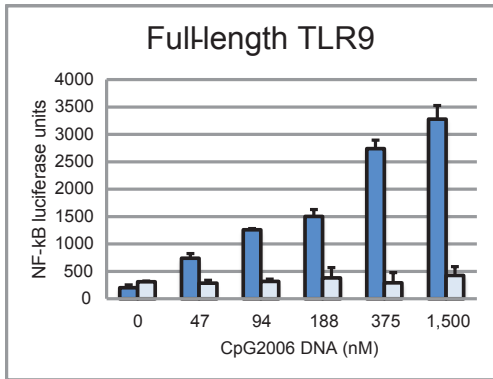


Figure 10

